Biophysical Chemistry, 47 (1993) 21–31
Elsevier Science Publishers B.V., Amsterdam

BIOCHE 01755

Fluorescence study of melanocyte stimulating hormones in AOT reverse micelles

Kasturi Bhattacharyya and Soumen Basak *

Nuclear Chemistry Division, Saha Institute of Nuclear Physics, 1/AF Bidhan Nagar, Calcutta - 700064 (India)

(Received 10 June 1992; accepted in revised form 14 January 1993)

Abstract

Fluorescence emission from the single tryptophan residues of two melanocyte stimulating hormones, α-MSH and δ-MSH, and their quenching kinetics were studied in aqueous solution and in reverse micelles of AOT/water/isooctane. Incorporation into micelles caused blue shifted and narrower emission peaks, altered quantum yields and considerably enhanced anisotropies for both peptides when compared to emission from bulk water. The variation of emission parameters with micellar water content was interpreted to suggest that while the tryptophan in α-MSH lies in close vicinity of the water–AOT molecular interface, that in δ-MSH is solubilized in the central water pool. Total emission intensity decays followed complex (biexponential) kinetics in both aqueous and micellar media. Although the mean lifetimes for both peptides were always nearly the same, the average rotational correlation times in micelles for α-MSH were three times as much as those for δ-MSH. Stern–Volmer plots obtained using acrylamide and CCl_4 as quenchers localized in the micellar and organic pseudophases, respectively, were non-linear and dependent on emission wavelength. Quenching by acrylamide was more efficient for δ-MSH than for α-MSH, while the opposite was true for quenching by CCl_4. The implication of this result for localization of the peptides in micelles was consistent with the earlier one emerging from these studies.

Keywords: Fluorescence; Quenching; Reverse micelles; Melanocyte stimulating hormones

1. Introduction

Peptide hormones are a class of short, biologically active peptides whose function is thought to depend on the secondary structures they adopt on binding with cell surface receptors. They exist in aqueous solution in multiple, rapidly interchanging conformational states and cannot generally be studied in their functional environment [1]. Thus there has been great interest in studies of peptide conformations in association with model interfaces, such as lipid vesicles, surfactant micelles and reverse micelles [2–4]. Of these the last mentioned offers the greatest flexibility and convenience of manipulation of the state of the interfacial water. The physical and chemical properties of this system vary extensively with its water-to-surfactant molar ratio w_0 (for literature reviews, see Refs. [3,4]). Macromolecules dissolved in the aqueous core of reverse micelles have been studied, using mostly spectroscopic methods, in varying states of hydration by follow-

* To whom correspondence should be addressed.

ing their behaviour as a function of the parameter w_0. Such studies report significant perturbations of conformation and associated characteristics of the molecules induced by the presence of surfactants, the extent of which depend on the charge state of surfactant head groups, water content of micelles and the nature of probe molecules [3–7].

α-Melanocyte stimulating hormone (α-MSH or α-melanotropin) is secreted by the intermediate lobe of vertebrate pituitaries and has been shown to act on adrenal cell steroidogenesis, pigment cell darkening and neural functioning related to learning and behaviour [8,9]. It is a linear tridecapeptide containing the first thirteen amino acids in the sequence of the larger pituitary hormone ACTH (adrenocorticotropic hormone), with which it shares a number of common hormonal properties. Its biologically active conformation has been proposed to contain a local structure (β-turn) within the "message" segment spanning residues 6–9 [10]. The heptapeptide δ-MSH, though lacking this sequence vital to the melanotropic activity of α-MSH, contains the residues Met, Glu and Trp at corresponding positions in its polypeptide chain, a significant difference being the presence of the fluorescent marker Trp at the very end of the chain in δ-MSH [11]. Their amino-acid sequences are as follows:

Ac–Ser–Tyr–Ser–Met–Glu–His–Phe–Arg–Trp
–Gly–Lys–Pro–Val–NH_2 (α-MSH)

Ser–Met–Glu–Val–Arg–Gly–Trp (δ-MSH)

We have used fluorescence spectroscopy to study two synthetic peptide hormones α-MSH and δ-MSH incorporated in reverse micelles of sodium dioctyl sulfosuccinate (AOT)/water/isooctane, which mimic the water–membrane interface well. The characteristics of steady-state emission from the single tryptophan residues of the peptides, and their excited-state lifetimes, were measured and compared with those of the model compound *N*-acetyl tryptophanamide (NATA). The kinetics of fluorescence quenching by two compounds of widely different hydrophobicities (acrylamide and carbon tetrachloride) were also measured to compare the relative locations of tryptophan fluorophores of the peptides in reverse micelles. Our results indicate that electrostatic interactions of charged amino-acid side chains with surfactant polar head groups play a key role in determining the localization of peptides.

2. Materials and methods

High purity α-MSH, δ-MSH, NATA, AOT and acrylamide were purchased from Sigma Chemical Co. (St. Louis, MO). Tetrachloromethane and isooctane (Uvasol grade) were from Merck (FRG). All chemicals were used as received. Purity of AOT was confirmed by the good agreement of its UV-absorption spectrum with that found in the literature [3].

Concentrated stock solutions of the compounds were prepared in pH 7.6, 0.05 *M* phosphate buffer. To incorporate each in micelles of a given w_0, the requisite volume (a few μl) of stock was injected into 1–2 ml of a 50 m*M* solution of AOT in isooctane, and shaken till clear [12]. During each series of experiments, w_0 was increased stepwise from 1.4 to 22.4 by adding further small aliquots of stock to the same AOT–isooctane solution. Optical densities of fluorescent samples at their excitation wavelengths were kept below 0.1.

Absorbances were measured on a Perkin-Elmer 554 spectrophotometer. Corrected emission spectra were recorded on a Hitachi 4010 spectrofluorometer, using excitation at 280 nm for δ-MSH and NATA and at 295 nm for α-MSH (to selectively excite its tryptophan residue). We found that excitation of the first two samples at 295 nm produced essentially the same w_0-dependence of fluorescence emission parameters as that found with 280 nm excitation, which indicates the absence of any complicating effects due to emission from the ^1L_a and ^1L_b states of indole [13]. Peptide-free micellar solutions of appropriate w_0 were used as reference blanks in absorbance measurements and for collecting baseline spectra in emission experiments. Typical excitation and emission bandwidths of (3, 1.5), (5, 5) and (3, 10) nm were used to measure wavelength

at emission maxima and bandwidth, quantum yield and steady-state anisotropy, respectively. All measurements, except as noted, were made at 20°C. The limiting anisotropy (r_0) was determined by extrapolating to zero the graph of $1/r$ versus T/η, obtained by measuring the anisotropy in a 90% glycerol–10% water mixture in the temperature range 30°C to −10°C.

Quantum yield of each peptide-containing micellar solution (ϕ_m) was determined relative to that (ϕ_{trp}) of a solution of L-tryptophan in pH 7.0 phosphate buffer, with ϕ_{trp} taken to be 0.14 [14,15]. These measurements were complicated by the fact that α-MSH was sparingly soluble in phosphate buffer (due probably to acetylation and amidation of the two ends of its peptide chain), which made the OD's of α-MSH-containing micellar solutions too small to be accurately measured, especially at low w_0. To circumvent this problem it was assumed that the OD's were proportional to w_0 (which was ensured by the method of preparation of micellar solutions of successively higher w_0), so that they could be determined relative to the OD of a high w_0 solution ($w_0 = 22.4$). For fluorometric titration of α-MSH the pH of an aqueous solution was adjusted by stepwise addition of minute amounts of concentrated HCl or NaOH.

Fluorescence total intensity decays were measured with an Edinburgh Instruments Model 199 time domain fluorometer using the single photon counting technique. Excitation at 297 nm was provided by a pulsed high pressure N_2 lamp operating at 25 kHz repitition rate, the pulse profile having a FWHM of 1.4 nanosecond. The decay profiles of all samples in buffer were collected at 350 nm, whereas in reverse micelles they were monitored at 337 nm, 350 nm and 340 nm for α-MSH, δ-MSH and NATA, respectively, using a bandwidth of 21.2 nm in all cases. Lifetimes were estimated by fitting to a single, or the sum of two, exponential decays using software supplied by manufacturers. Best-fit values of lifetimes, as judged by minima of χ^2, were accepted.

Quenching experiments on each sample were performed by serially adding small aliquots (i.e., 2–4 μl) of a very concentrated quencher solution (typically 4 *M* acrylamide or CCl_4 stock) to about 1 ml of the sample in a cuvette, mixing and measuring the fluorescence intensity with 295 nm excitation. Corrections were applied for dilution of the fluorescent material and for absorption of incident light by acrylamide, this being minimal at 295 nm [16]. Quenching data were fitted to a modified form of the Stern–Volmer equation by using non-linear least-squares analysis [17]:

$$\frac{F_0}{F_{corr}\, e^{V[Q]}} = 1 + K_{SV}[Q] \qquad (1)$$

where F_{corr} is the intensity corrected for acrylamide absorption, [Q] the quencher concentration, K_{SV} the Stern–Volmer (dynamic quenching) constant, and V is known as the static quenching constant.

3. Results

3.1. Emission maxima and bandwidths

Steady-state fluorescence emission spectra of the peptides in buffer showed single peaks characteristic of tryptophan residues exposed to the aqueous environment, as evidenced by the close similarity of their location (λ_m) and bandwidth ($\Delta\lambda$ = FWHM) with those of the emission maximum of NATA (see Table 1). Upon incorporation of the peptides into reverse micelles the emission peaks were blue shifted and their bandwidths were reduced, as shown in Figs. 1(a) and 1(b). Similar changes in emission parameters have been reported for a number of peptide hormones and their fragments solubilized in reverse micelles [6]. Of the three samples α-MSH showed the largest blue shift and peak sharpening while δ-MSH showed the least, these effects being the most prominent for w_0 between 1.4 and 8 and decreasing significantly above $w_0 \approx 10$. The emission spectrum of δ-MSH in reverse micelles of the highest w_0 (= 22.4) had characteristic parameters ($\lambda_m = 351$ nm, $\Delta\lambda = 60$ nm) almost identical to those of its spectrum in aqueous solution. By contrast, the values of these parameters for α-MSH ($\lambda_m = 337$ nm, $\Delta\lambda = 56$ nm) and NATA ($\lambda_m = 344$ nm, $\Delta\lambda = 57$ nm) in micelles (at $w_0 =$

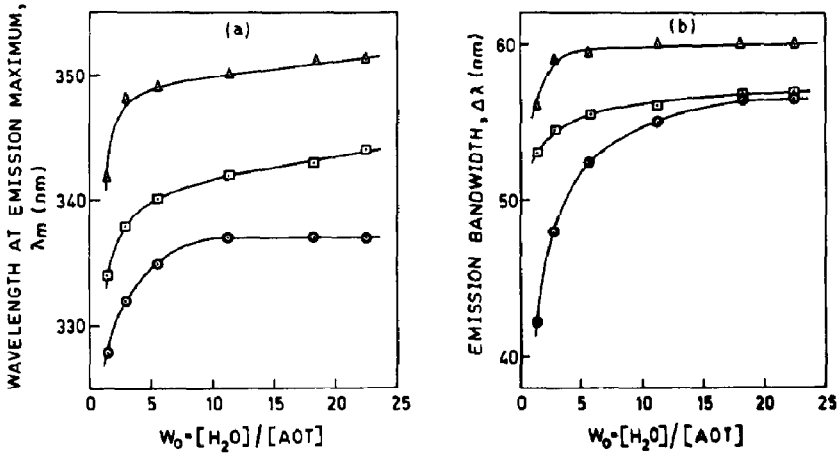

Fig. 1. Variation of (a) wavelength (λ_m) and (b) bandwidth ($\Delta\lambda$) of emission maxima with micellar water content (w_0) for α-MSH (⊙), δ-MSH (▲) and NATA (□).

22.4) differed distinctly from their corresponding values in water (Table 1).

3.2. Quantum yield

In micelles of low w_0 ($\lesssim 3$) the quantum yields of all three samples were higher than in aqueous solution, decreasing with increasing w_0 as shown in Fig. 2. As with λ_m and $\Delta\lambda$, the relative change of the yields with w_0 slowed down appreciably for $w_0 \gtrsim 10$. However, a qualitative difference was observed between the w_0-dependence of the yields of δ-MSH on the one hand and of α-MSH and NATA on the other. For δ-MSH the quantum yield in reverse micelles of all w_0 was higher than that in bulk water. For α-MSH and NATA the yields in micelles dropped below their respective values in aqueous solution for $w_0 \gtrsim 3$.

The inset of Fig. 2 shows the result of a fluorometric titration of α-MSH in the pH range 4–9, the ratio of the peak emission intensity to the absorbance at the excitation wavelength (295 nm) being plotted along the y-axis. The data point to the presence of a quenching mechanism in α-MSH which involves interaction of its tryptophan with some such ionizable group as histidine ($pK_a = 6.5$).

Table 1

Summarized steady-state emission parameters of α-MSH, δ-MSH and NATA in 0.05 M, pH 7.6 phosphate buffer

Compound	λ_m (nm)	$\Delta\lambda$ (nm)	ϕ	r [a]	r_0
α-MSH	350	60	0.07	0.025	0.207
δ-MSH	355	61	0.09	0.014	0.196
NATA	354	60	0.14	0.0	0.181

[a] Excitation wavelength 295 nm.

3.3. Fluorescence decay lifetimes

Time-resolved measurements of tryptophan emission intensity from the peptides, both in

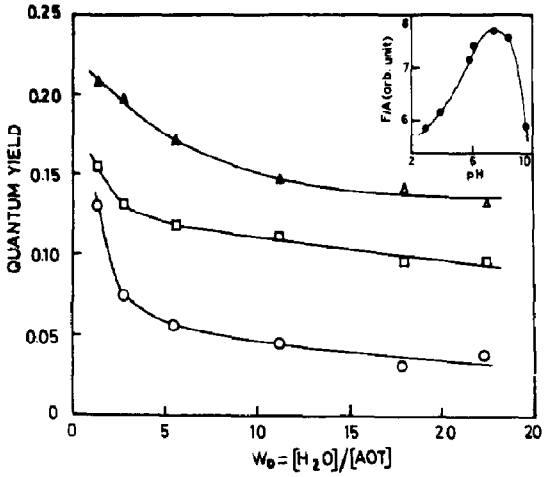

Fig. 2. Variation of quantum yield with w_0 (symbols as in Fig. 1). The inset shows the dependence on pH of the fluorescence intensity at the emission peak of α-MSH divided by its absorbance at the excitation wavelength, this ratio being proportional to the quantum yield [25].

aqueous solution and in reverse micelles of w_0 = 5.6, 11.2 and 22.4, showed good fits to biexponential decays as judged by χ^2-minimization and deviation function criteria. The best-fit parameters—lifetime components (τ_i) and amplitudes (α_i)—are listed in Table 2. The two lifetime components lie around 1 ns and between 3–4 ns, in general agreement with the their values found for tryptophan in the free state and in similar peptides [6,18]. Although both individual components for the micellized peptides decreased with increasing w_0, their relative amplitudes varied in such manner as to produce only a small decrease of the mean lifetime $\langle\tau\rangle$ ($=\alpha_1\tau_1+\alpha_2\tau_2$) for α-MSH and a similar increase for δ-MSH over the range of w_0 studied. For NATA, a monoexponential was found to be sufficient for good fits to the fluorescence intensity decays, both in water and in reverse micelles of $w_0 = 22.4$. The lifetimes so obtained were in good agreement with the mean lifetimes obtained for NATA under similar conditions by other investigators [6,7].

3.4. Steady-state anisotropy

In aqueous solution both peptides exhibited low values of the anisotropy measured at 295 nm excitation. Incorporation into reverse micelles substantially increased the anisotropy, especially at low w_0, and at 20°C gave rise to excitation anistropy spectra (see Ref. [19]) similar in size and shape to that reported for trp in viscous solvents at low temperatures [13]. For α-MSH the anisotropy remained more or less constant as w_0 increased from 5.6 to 22.4, whereas for δ-MSH and NATA it decreased by 20% over this range (Fig. 3). Using this data and the mean lifetimes in

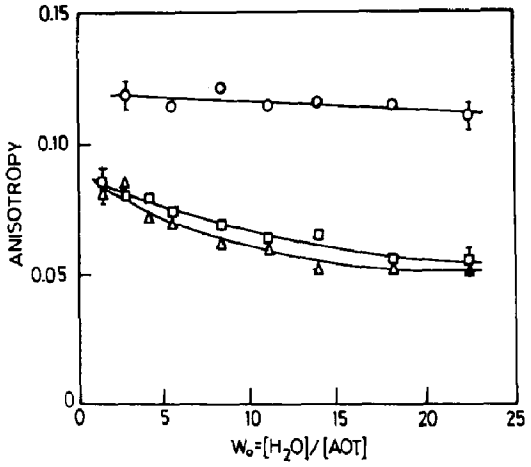

Fig. 3. Variation of steady-state anisotropy (at 295 nm excitation) with w_0, calculated after subtracting AOT/isooctane baseline contributions for each setting of polarizers. Error bars represent the spread in results of several measurements on the same sample. Symbols as in Fig. 1. Solid lines show only the trend of data.

Table 2

Fluorescence lifetimes of the peptides and NATA in different media. Excitation was at 297 nm for all three samples. Total intensity decay profiles collected at respective emission peaks were fitted to the expression $I(t)=\alpha_1\exp(-t/\tau_1)+\alpha_2\exp(-t/\tau_2)$ for the peptides; for NATA, a single exponential sufficed to give good fits to the observed decays. Mean lifetimes were calculated using $\langle\tau\rangle=\alpha_1\tau_1+\alpha_2\tau_2$. Estimated errors were ±0.1 ns

Sample	Medium w_0	τ_1 (ns)	α_1	τ_2 (ns)	α_2	$\langle\tau\rangle$ (ns)	τ_c (ns)
α-MSH	5.6	4.5	0.42	1.4	0.58	2.7	3.3
	11.2	4.4	0.43	1.3	0.57	2.6	3.2
	22.4	3.2	0.61	0.9	0.39	2.3	2.7
	Buffer	3.2	0.73	0.9	0.27	2.6	0.36
δ-MSH	5.6	4.0	0.39	1.3	0.61	2.4	1.2
	11.2	3.8	0.52	1.3	0.48	2.6	1.2
	22.4	3.7	0.77	0.8	0.23	3.0	1.2
	Buffer	3.2	0.85	1.1	0.15	2.9	0.22
NATA	22.4	2.0	1.0			2.0	1.0
	Buffer	3.0	1.0			3.0	0.0

Table 2, average rotational correlation times (τ_c) were calculated using Perrin's equation [20]:

$$\tau_c = \langle\tau\rangle/(r_0/r - 1) \quad (2)$$

where r_0 is the limiting anisotropy for the peptides, determined by extrapolation of $1/r$ vs. T/η graphs as described above (Table 1). The values of τ_c, so calculated (Table 2), were between five (for δ-MSH) to ten (for α-MSH) times larger in micelles than in aqueous solution. In micelles, τ_c for α-MSH decreased from 3.8 ns at $w_0 = 5.6$ to 3.3 ns at $w_0 = 22.4$, whereas for δ-MSH it remained constant at 1.2 ns throughout this range. For NATA, τ_c at $w_0 = 22.4$ had nearly this same value.

3.5. Fluorescence quenching

Stern–Volmer plots for quenching by CCl_4 and acrylamide, both in aqueous solution and in reverse micelles, showed upward curvature for both peptides and NATA (Figs. 4–6). Such nonlinear plots indicate the presence of a static quenching mechanism, as shown explicitly from lifetime measurements for NATA and other indolic compounds in water and in association with SDS micelles [16]. Values of K_{SV} and V obtained by fitting the data to a modified Stern–Volmer equation (eq. 1) are collected in Table 3. Using the mean lifetimes in Table 2, bimolecular rate contants ($k_q = K_{SV}/\langle\tau\rangle$) for acrylamide quenching of the peptides in water come out close to the value ($6 \times 10^9\ M^{-1}\ s^{-1}$) measured for free tryptophan [16].

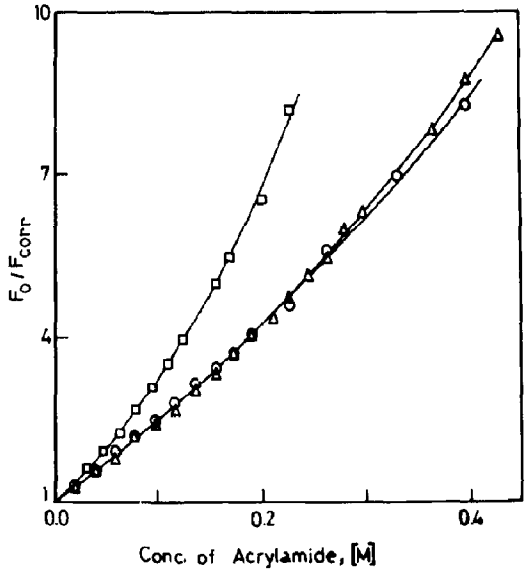

Fig. 4. Quenching of fluorescence from α-MSH (○), δ-MSH (△) and NATA (□) by acrylamide in buffer, monitored at 350 nm emission. The solid lines represent fits of data to eq. (1) of the text.

Table 3

Quenching rate constants obtained by fitting data in Figs. 4–6 to the modified Stern–Volmer equation: $F_0/F_{corr}e^{V[Q]} = 1 + K_{SV}[Q]$. Units are M^{-1} for V and K_{SV} and $10^9\ M^{-1}\ s^{-1}$ for k_q. Estimated limits of error in K_{SV} and V are ±10% and ±20%, respectively. The normalized accessibility factor (*naf*) of acrylamide for a sample was calculated as the ratio of its k_q (averaged over three wavelengths) in reverse micelles to that in bulk water [27]

Wavelength (nm)	Sample											
	α-MSH				δ-MSH				NATA			
	V	K_{SV}	k_q	*naf*	V	K_{SV}	k_q	*naf*	V	K_{SV}	k_q	*naf*
Acrylamide quenching in water												
350	0.67	13.7	5.27		0.93	12.7	4.38		2.68	15.0	4.84	
Acrylamide quenching in reverse micelles												
340	0.63	0.63	0.27		0.47	2.69	0.90		0.76	1.27	0.64	
350	0.64	0.82	0.36	0.07	0.54	2.74	0.91	0.21	0.86	1.22	0.61	0.13
360	0.74	0.96	0.42		0.60	2.83	0.94		0.93	1.20	0.60	
Carbon tetrachloride quenching in reverse micelles												
340	2.50	3.90	1.70		0.88	2.50	0.83		1.77	2.44	1.22	
350	1.98	4.17	1.81		0.51	2.68	0.89		1.56	2.65	1.33	
360	1.17	5.17	2.25		0.15	2.85	0.95		1.34	2.75	1.38	

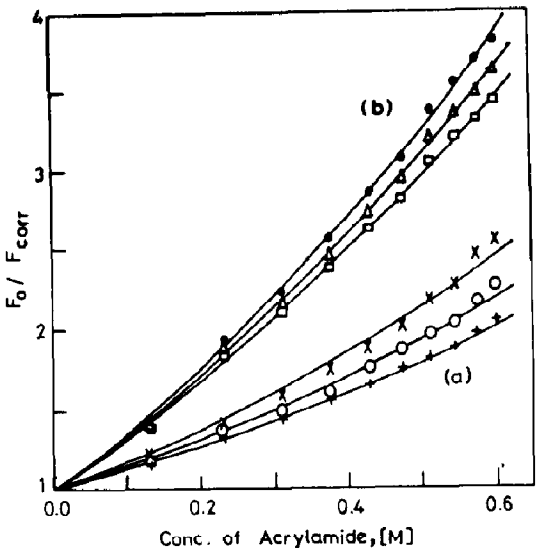

Fig. 5. Fluorescence quenching by acrylamide of peptides in reverse micelles (at $w_0 = 22.4$), showing dependence on emission wavelength: (a) α-MSH at 340 nm (+), 350 nm (○) and 360 nm (×); (b) δ-MSH at 340 nm (□), 350 nm (△) and 360 nm (●). Solid lines represent fits to eq. (1) of text.

The efficiencies of both quenchers were considerably lower in reverse micelles, and wavelength dependences of quenching were evident

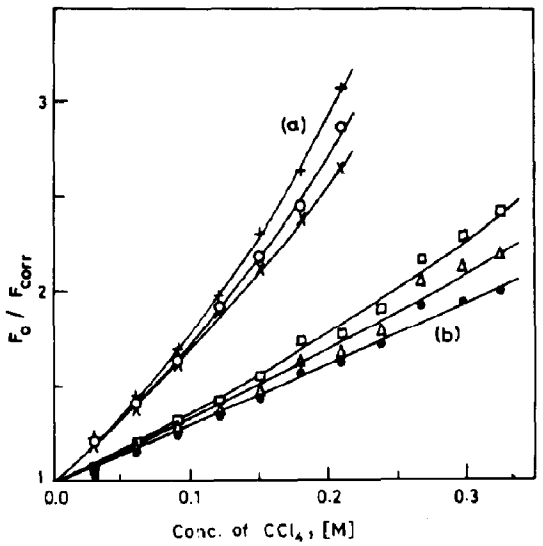

Fig. 6. Fluorescence quenching by carbon tetrachloride of peptides in reverse micelles ($w_0 = 22.4$), showing dependence on emission wavelength; symbols as in Fig. 5. Solid lines are fits to eq. (1) of text.

(Table 3, Figs. 5 and 6). Control experiments were performed to detect if acrylamide quenching in buffer also showed any wavelength dependence. However, quenching plots at the three wavelengths were indistinguishable from one another on the scale of Fig. 4. Fits of these data to eq. (1) yielded values of K_{SV} and V varying randomly by 2–4% with wavelength. This variation is at least an order of magnitude smaller than that observed for quenching in micelles (Table 3), and imply the absence of wavelength dependent quenching in bulk water.

To enable comparison of the residual accessibility of the two peptides to the aqueous quencher acrylamide we calculated the normalized accessibility factor (*naf*), defined as the ratio of the quenching constant (k_q) in micelles to that in water [21]. These are also listed in Table 3. It is clear from the *naf* values that in reverse micelles the relative accessibility of acrylamide for δ-MSH is 3 times that for α-MSH. Table 3 also shows that the rate constants (k_q) for quenching of micelle-incorporated α-MSH by CCl_4 are more than twice as much as they are for δ-MSH.

For the peptides, static quenching contributions (V) by both agents were throughout small (Table 3), but a nearly threefold increase was observed for CCl_4 quenching of α-MSH in micelles when compared to its quenching by acrylamide in the same environment. As the static quenching mechanism is short-ranged and non-diffusive, i.e., viscosity-independent, this result implies a higher effective concentration of CCl_4 than acrylamide around α-MSH in the micelles [16].

Another interesting result that emerges from these studies is that acrylamide and CCl_4 play opposite roles as regards the wavelength dependence of quenching efficiency, namely, that acrylamide quenches the peptide fluorescence more efficiently at higher emission wavelengths, whereas CCl_4 quenches it more efficiently at lower wavelengths. These can be inferred from the data shown in Figs. 5 and 6, as well as from the corresponding values of K_{SV} and V in Table 3. Such wavelength dependent quenching by acrylamide and CCl_4, and the complementary nature of the effects produced by these two

agents, have previously been reported for a series of indole derivatives in AOT/n-heptane reverse micelles [22,23].

Stern–Volmer plots for quenching of the control compound NATA in reverse micelles always fell between those obtained for the two peptides, and showed wavelength dependence similar to that observed for δ-MSH (Table 3). Values of K_{SV} for acrylamide quenching of NATA were in between those for the peptides, while V had values of the same order for all.

4. Discussion

The fluorescence behaviour of the peptides in micelles differ markedly from that in aqueous solution and strongly depend on the amount of water present in the micelles. The main features of the results shown in Figs. 1–3 can be explained by restricted capabilities for relaxation of the peptide side chains, and for reorientation of the solvent molecules, in the micellar interior [6,20]. Experiments have generally confirmed the existence of two distinct populations of water in reverse micelles: surfactant "bound" (interfacial) and "bulk" water, the latter developing as hydration of the surfactant headgroups and counterions becomes complete with increasing micellar water content (by various methods of estimation, this occurs at $w_0 \gtrsim 10$). At low w_0 the first type of water predominates, with the result that solvated molecules experience a rigidly structured aqueous environment of low polarizability and high microviscosity. The blue shifts and reduced bandwidths of the emission peaks, and enhancement of the quantum yields and steady-state anisotropies reported here, are all consequences of the altered hydration states of the fluorophores in micelles [4–7]. The fact that these parameters assume values approaching those typical of the aqueous medium for $w_0 \gtrsim 10$ is indicative of a bulk-like water pool beginning to form. In this context, then, it is significant that the saturation values of the emission parameters λ_m and $\Delta\lambda$ in micelles differ considerably from those in bulk water for α-MSH but not for δ-MSH. This result points to a difference in the sites of localization of their tryptophan residues: the trp in α-MSH is preferentially located near the micellar interface, while the one in δ-MSH is displaced toward the central pool by addition of water.

One aspect of the quantum yield data of Fig. 2 merits discussion. As the micellar water is less polar and more rigidly structured than bulk water even at $w_0 = 22.4$, quantum yields of solubilized probes are expected to diminish with increasing w_0 but nevertheless should remain higher than their respective values in aqueous solution [14]. The departure from such behaviour in the case of α-MSH and NATA suggests the existence of additional deactivation pathways for the excited states of these two molecules that do not play a significant role for δ-MSH. A relevant quenching mechanism was suggested by Ricci and Nesta from observations of quenching of indole fluorescence by carbonyl compounds [24]. They attributed it to formation of an excited-state charge transfer complex between indole and a carbonyl group in which the former acts as a donor. Thus the effect in question is likely due to quenching by the carbonyl groups of surfactants. Closer proximity of α-MSH to the micellar interface (compared to δ-MSH) can lead to higher probability of encounter between its indole ring and the AOT carbonyls, causing more effective quenching of its emission.

It is also worth considering the implication of the pH titration curve of α-MSH (inset, Fig. 2) for its quantum yield behaviour in reverse micelles. The single histidine residue in α-MSH, located three residues away from its tryptophan, most likely quenches the trp excited singlet state below pH 6 by a proton transfer mechanism [25]. It is conceivable that the restricted environment of the micellar interior stabilizes the α-MSH chain into a conformation in which these two residues interact more strongly and for longer periods than in water, where such peptides are known to exist in extended, flexible conformations with almost no ordered structure. This quenching mechanism may then contribute to the marked decrease of quantum yield of α-MSH in micelles.

The simple exponential decay of the total emission intensity from NATA, both in water and in reverse micelles (of $w_0 = 22.4$), represents the

limiting case of fluorophore in a solvent-relaxed environment. Further evidence for this is provided by the fact that the fluorescence rate constant (k_f) of indole, as obtained from the ratio of quantum yield to lifetime for NATA, was constant in going from water (0.045) to the micelles (0.048) and had about the same value as that found for a number of indole derivatives in water exhibiting single exponential decay [26]. In contrast, time-resolved intensity data for the MSH peptides both in aqueous and micellar media yield complex kinetics which could be fitted to biexponential decays and gave rise to wide variations in the rate constant k_f. Other investigators have found the decay parameters (α_i and τ_i) of similar flexible polypeptides and peptide fragments in water to be wavelength independent across the emission spectrum and have used this result to argue that complex decays in these peptides are due to a distribution of slightly different tryptophan environments in the ground state [6,27]. Different degrees of quenching of the indole excited state would lead to a distribution of fluorescence decay times, and hence multiexponential decay kinetics. In the present case, the close similarity of the lifetime components for the MSH peptides suggests that interaction of the trp with near-neighbour amino acids exerts the main influence on its emission kinetics. The guanidinium quenching group of the nearby arginine in both peptides is likely of primary importance in this respect, as suggested by Ross et al. [27].

Upon incorporation of the peptides in reverse micelles, their trp side chains are constrained to rotate within a restricted volume of the ordered peptide matrix, which in turn sets up rotational barriers to trp motion in the nanosecond time scale and leads to complex decay kinetics [28]. This also increases the steady-state anisotropy considerably. The average rotational correlation times in micelles for α-MSH are about thrice as much as for δ-MSH (Table 3). Anisotropy decay measurements have previously indicated that rotational motions of the trp fluorophore are characterized by two correlation times differing by at least an order of magnitude [6]. The short correlation time (in the neighbourhood of 1 ns) represents the tumbling of the solute within the micellar water pool, while the longer component (≈ 10 ns) corresponds to rotational diffusion of the micelle itself. The τ_c calculated from Perrin's equation must be an appropriate average of these two components. Since the longer component is likely to be determined by the size and water content of the micelles, the almost triple values of τ_c for α-MSH compared to δ-MSH points to a considerably greater degree of restraint imposed on trp side chain rotations of α-MSH by the micellar environment. It also implies a stronger coupling between the two rotational motions of α-MSH arising out of stronger interactions of this peptide with the AOT sulfonate groups and the structured interfacial water layer in which it is likely to be embedded. The τ_c values for δ-MSH and NATA are nearly the same in spite of the difference in the sizes of these two molecules, implying the close similarity of their trp environments and fluorophore–water interactions.

Fluorescence quenching experiments can lead to information about the relative positions of indole moieties in reverse micelles, when quenchers having affinities specifically for the aqueous and hydrocarbon phases are used. Although the inherent heterogeneity of the host system in the present case results in a heterogeneous distribution of probe and quencher in micelles, acrylamide can be considered confined to the water pool and the interfacial region, while the uptake of CCl_4 by AOT has been shown to be negligible [22]. Study of the *naf* values for quenching of the peptides (Table 3) points to a comparatively higher accessibility of the aqueous quencher acrylamide to δ-MSH, in parallel with reduced accessibility of the hydrophobic agent CCl_4 to this peptide, and confirms the relatively distinct regions of localization of the two peptides within reverse micelles. The static quenching contributions (represented by the term $e^{V[Q]}$), which increase with quencher concentration around the fluorophore, similarly suggest a higher concentration of CCl_4 around the trp of α-MSH. This raises the possibility of the trp side chain being inserted into the hydrophobic tail region of the AOT boundary layer.

The wavelength-dependent quenching results in micelles can be understood if we assume the

excited fluorophores to be distributed among several different environments, with the rates of interchange between these positions being slower than excited state decay [22,23]. The molecules nearer to the isooctane phase will then fluoresce predominantly at shorter wavelengths and be more prone to quenching by CCl_4, while those located nearer (or inside) the water pool will emit at longer wavelengths and be preferentially deactivated by acrylamide. This reasoning assumes partitioning of acrylamide and CCl_4 into the micellar and hydrocarbon phases, respectively, to account for their complementary wavelength dependences of quenching. It also raises the interesting possibility that heterogeneity of tryptophan environment, which presumably is the source of wavelength dependent quenching, may be studied by following the wavelength dependence of fluorescence lifetimes of the peptides in micelles [27].

5. Conclusions

In view of the implications it may have for peptide conformations in biomimetic environments, it is worth considering the physical reason behind the principal result of this work, namely, that the two peptides have tendencies for localization in different regions inside AOT reverse micelles. The origin of this difference appears to lie in the electrostatic interaction between positively charged side chains (Arg and Lys) of α-MSH and negatively charged headgroups (sulfonate) of AOT, which attributes this peptide with affinity for the micellar interface. The hydrophobic character of the trp side chain can lead to its insertion into the hydrocarbon tails of the surfactants, while the charged residues on either side keep it anchored in this position. Similar considerations may be responsible for the observed location of α-MSH at the boundaries of phospholipid vesicles [21] and for the generation of a secondary structure in the biologically active conformation of α-MSH [10]. As δ-MSH is electrically neutral, its trp is free from the attractive influence of the interface and prefers to populate the micellar centre, where the comparatively mobile water molecules provide a relaxed solvent environment. The location of this trp at the C-terminus of the peptide chain reduces its hydrophobic character and also helps localize it in the polar water pool.

Acknowledgements

The authors wish to express their sincere thanks to Professor S.C. Bera and Dr. N. Chatterjee for extending them the facilities for fluorescence lifetime measurements reported here. They also express thanks to Professors S.N. Bhattacharyya, S.K. Ghosh and D. Dasgupta for useful discussions.

References

1 T. Blundell and S. Wood, Annu. Rev. Biochem. 51 (1982) 123.
2 J.W. Taylor and G. Ösapay, Acc. Chem. Res. 23 (1990) 338.
3 P.L. Luisi and L.J. Magid, Crit. Rev. Biochem. 20 (1986) 409.
4 M. Waks, Proteins Struct. Function Genet. 1 (1986) 4.
5 C. Nicot, M. Vacher, M. Vincent, J. Gallay and M. Waks, Biochemistry 24 (1985) 7024.
6 J. Gallay, M. Vincent, C. Nicot and M. Waks, Biochemistry 26 (1987) 5738.
7 S. Ferreira and E. Gratton, J. Mol. Liq. 45 (1990) 253.
8 R. Schwyzer, Ann. N.Y. Acad. Sci. 297 (1977) 3.
9 R. Schwyzer, Helv. Chim. Acta 69 (1986) 1685.
10 T.K. Sawyer, V.J. Hruby, P.S. Darman and M.E. Hadley, Proc. Natl. Acad. Sci. U.S.A. 79 (1982) 1751.
11 S. Nakanishi, A. Inoue, T. Kita, M. Nakamura, A.C.Y. Chang, S.N. Cohen and S. Numa, Nature 278 (1979) 423.
12 C. Grandi, R.E. Smith and P.L. Luisi, J. Biol. Chem. 256 (1981) 837.
13 B. Valeur and G. Weber, Photochem. Photobiol. 25 (1977) 441.
14 M. Wong, J.K. Thomas and M. Gratzel, J. Am. Chem. Soc. 98 (1976) 2391.
15 O. Wolfbeis, in: Molecular luminescence spectroscopy, Part I, ed. S. Schulman (Wiley, New York, 1985) p. 167.
16 M.R. Eftink and C.A. Ghiron, J. Phys. Chem. 80 (1976) 486.
17 P.R. Bevington, Data reduction and error analysis for the physical sciences (McGraw Hill, New York, 1969).
18 L.X.-Q. Chen, J.W. Petrich, G.R. Fleming and A. Perico, Chem. Phys. Lett. 139 (1987) 55.
19 K. Bhattacharyya and S. Basak, Ind. J. Phys. 65B (1991) 481.

20 J.R. Lakowicz, Principles of Fluorescence Spectroscopy (Plenum, New York, 1983).
21 A. de Kroon, J. de Gier and B. de Kruijff, Biochim. Biophys. Acta 1068 (1991) 111.
22 E.A. Lissi, M.V. Encinas, S.G. Bertolotti, J.J. Cosa and C.M. Previtali, Photochem. Photobiol. 51 (1990) 53.
23 M.V. Encinas, E.A. Lissi, S.G. Bertolotti, J.J. Cosa and C.M. Previtali, Photochem. Photobiol. 52 (1990) 981.
24 R.W. Ricci and J.M. Nesta, J. Phys. Chem. 80 (1976) 974.
25 M. Shinitzky and R. Goldman, Eur. J. Biochem. 3 (1967) 139.
26 T.C. Werner and L.S. Forster, Photochem. Photobiol. 29 (1970) 905.
27 J.B.A. Ross, K.W. Rousslang and L. Brand, Biochemistry 20 (1981) 4361.
28 P.H. Wahl, Chem. Phys. 7 (1975) 220.